similar function in all evergreen leaves, irrespective of their longevity. In fact, studies across biomes with different evolutionary and climatic histories demonstrate that this categorization is unlikely to be correct because leaf lifespan is strongly correlated with physiological, whole-tree and ecosystem processes[14,25,26]. A palaeontological view of leaf lifespan is now afforded through anatomical analyses of growth rings in fossil woods[27], providing a critical means of linking past and present forest physiology. □

Methods

Whole-tree CO_2 flux measurements

The net carbon exchange rates of trees were tracked throughout the year under growth conditions using eight custom-built chambers, based on a modified design of ref. 28. Three replicate plants per CO_2 treatment were used, and the remaining two chambers used for controls, one from each CO_2 treatment, consisting of a pot with the same soil mixture as those with plants. Hourly measurements were made for each species over the course of a 24-h period, and repeated ten times throughout the year. Daily carbon budgets were estimated from the resulting 400 measurements, and then integrated to produce annual budgets (NPP) after taking into account the annual carbon loss by litter production. The carbon contribution of litter was estimated in sub-samples of leaf litter, using a stable-isotope ratio mass spectrometer (PDZ Europa 20–20, Cheshire).

CO_2 effects were analysed using a two-way ANOVA with replication (CO_2 × species); leaf habit effects were analysed using a two-way ANOVA with unequal but proportional subclass sizes (CO_2 × leaf habit) (ref. 29). None had significant interaction terms.

Scaling experimental results to mature stands

The following values for τ and measured LCD (mean ± s.e.) were used: for *N. cunninghamii* (at 400 p.p.m.v. CO_2: $\tau = 0.33$, LCD = 51.2 ± 2.6; at 800 p.p.m.v. CO_2: 0.33, 56.2 ± 7.1), for *S. sempervirens* (at 400 p.p.m.v. CO_2: 0.2, 44.0 ± 3.8; at 800 p.p.m.v. CO_2: 0.2, 70.1 ± 12.5), for *M. glyptostroboides* (at 400 p.p.m.v. CO_2: 1.0, 34.1 ± 2.6; at 800 p.p.m.v. CO_2: 1.0, 42.3 ± 3.0), for *T. distichum* (at 400 p.p.m.v. CO_2: 1.0, 53.0 ± 3.3; at 800 p.p.m.v. CO_2: 1.0, 60.4 ± 10.3) and for *G. biloba* (at 400 p.p.m.v. CO_2: 1.0, 38.9 ± 2.8; 800 p.p.m.v. CO_2: 1.0, 52.0 ± 1.7). See Fig. 2a for canopy respiration data (R). Measured rates of belowground respiration did not differ significantly between the two leaf habits during the polar winter ($F_{1,6} = 0.32$, $P = 0.59$), and so were not included in the scaling procedures.

Conifer forest modelling

The University of Sheffield Conifer Model (USCM) uses generalized relationships between leaf lifespan and function, and incorporates a full set of responses to atmospheric CO_2 and climate, as well as feedbacks with soil water and nutrient content[14]. USCM predictions of key properties and processes of conifer forests (NPP, LAI, evapotranspiration, nitrogen uptake and carbon partitioning) are validated well for forest sites across a wide climatic gradient using monthly climate data (temperature, precipitation and relative humidity), soil nutrient status and leaf lifespan information as inputs[14]. We forced the USCM with monthly climate data from the mid-Cretaceous climate simulation by the UK Universities Global Atmospheric Modelling Programme general circulation model[19]. Soil nutrient data for the Cretaceous period were derived using the Century soil biogeochemistry routines[30].

Received 28 February; accepted 22 April 2003; doi:10.1038/nature01737.

1. Spicer, R. A. & Chapman, J. L. Climate change and the evolution of high-latitude terrestrial vegetation and flora. *Trends Ecol. Evol.* **5,** 279–284 (1990).
2. Crowley, T. J. & Berner, R. A. CO_2 and climate change. *Science* **292,** 870–872 (2001).
3. Seward, A. C. Antarctic Fossil Plants. British Antarctic ('Terra Nova') Expedition, 1910. *British Museum Natural History Report. Geology* **1,** 1–49 (1914).
4. Chaney, R. W. Tertiary centers and migration routes. *Ecol. Monogr.* **17,** 139–148 (1947).
5. Hickey, L. J. Eternal summer at 80 degrees north. *Discovery* **17,** 17–23 (1984).
6. Wolfe, J. A. in *The Carbon Cycle and Atmospheric CO_2: Natural Variations, Archean to Present* (eds Sundquist, E. T. & Broecker, W. S.) 357–375 (Geophys. Monogr. Ser. 32, American Geophysical Union, Washington DC, 1985).
7. Falcon-Lang, H. J. & Cantrill, D. J. Leaf phenology of some mid-Cretaceous polar forests, Alexander Island, Antarctica. *Geol. Mag.* **138,** 39–52 (2001).
8. Estes, R. & Hutchison, J. Eocene lower vertebrates from Ellesmere Island, Canadian Arctic Archipelago. *Palaeogeogr. Palaeoclimatol. Palaeoecol.* **30,** 325–347 (1980).
9. Tarduno, J. A. *et al.* Evidence for extreme climatic warmth from Late Cretaceous arctic vertebrates. *Science* **282,** 2241–2244 (1998).
10. Tripati, A., Zachos, J., Marincovich, L. & Bice, K. Late Paleocene Arctic coastal climate inferred from molluscan stable and radiogenic isotope ratios. *Palaeogeogr. Palaeoclimatol. Palaeoecol.* **170,** 101–113 (2001).
11. Dutton, A. L., Lohmann, K. C. & Zinsmeister, W. J. Stable isotope and minor element proxies for Eocene climate of Seymour Island, Antarctica. *Paleoceanography* **17**(2), 1016, doi:10.1029/2000PA000593 (2002).
12. Müller, M. J. *Selected Climatic Data for a Global Set of Standard Stations for Vegetation Science* (Kluwer Academic, Dordrecht, The Netherlands, 1981).
13. Beerling, D. J. & Osborne, C. P. Physiological ecology of Mesozoic polar forests in a high CO_2 environment. *Ann. Bot.* **89,** 329–339 (2002).
14. Osborne, C. P. & Beerling, D. J. A process-based model of conifer forest structure and function with special emphasis on leaf lifespan. *Glob. Biogeochem. Cycles* **16**(4), 1097 doi:10.1029/2001GB001467 (2002).
15. Tjoelker, M. G., Oleksyn, J. & Reich, P. B. Modelling respiration of vegetation: evidence for a general temperature-dependent Q_{10}. *Glob. Change Biol.* **7,** 223–230 (2001).
16. Read, J. & Francis, J. Responses of some Southern Hemisphere tree species to a prolonged dark period and their implications for high-latitude Cretaceous and Tertiary floras. *Palaeogeogr. Palaeoclimatol. Palaeoecol.* **99,** 271–290 (1992).
17. Villar, R. & Merino, J. Comparison of leaf construction costs in woody species with differing leaf lifespans in contrasting ecosystems. *New Phytol.* **151,** 213–226 (2001).
18. Yin, X. Responses of leaf nitrogen concentration and specific leaf area to atmospheric CO_2 enrichment: a retrospective synthesis across 62 species. *Glob. Change Biol.* **8,** 631–642 (2002).
19. Valdes, P. J., Sellwood, B. W. & Price, G. D. Evaluating concepts of Cretaceous equability. *Palaeoclim. Data Modell.* **2,** 139–158 (1996).
20. Creber, G. T. & Chaloner, W. G. Tree growth in the Mesozoic and Early Tertiary and the reconstruction of palaeoclimates. *Palaeogeogr. Palaeoclimatol. Palaeoecol.* **52,** 35–60 (1985).
21. Upchurch, G. R. & Askin, R. A. Latest Cretaceous and earliest Tertiary dispersed plant cuticles from Seymour Island. *Antarct. J. US* **24,** 7–10 (1990).
22. Parrish, J. T., Daniel, I. L., Kennedy, E. M. & Spicer, R. A. Paleoclimatic significance of mid-Cretaceous floras from the middle Clarence Valley, New Zealand. *Palaios* **13,** 149–159 (1998).
23. Axelrod, D. I. Origin of deciduous and evergreen habits in temperate forests. *Evolution* **20,** 1–15 (1966).
24. Wolfe, J. A. Late Cretaceous-Cenozoic history of deciduousness and the terminal Cretaceous event. *Paleobiology* **13,** 215–226 (1987).
25. Reich, P. B., Walters, M. B. & Ellsworth, D. S. From tropics to tundra: global convergence in plant functioning. *Proc. Natl Acad. Sci. USA* **94,** 13730–13734 (1997).
26. Givnish, T. J. Adaptive significance of evergreen vs. deciduous leaves: solving the triple paradox. *Silva Fennica* **36,** 703–743 (2002).
27. Falcon-Lang, H. J. The relationship between leaf longevity and growth ring markedness in modern conifer woods and its implications for palaeoclimatic studies. *Palaeogeogr. Palaeoclimatol. Palaeoecol.* **160,** 317–328 (2000).
28. Beerling, D. J. *et al.* The influence of Carboniferous palaeoatmospheres on plant function: an experimental and modelling assessment. *Phil. Trans. R. Soc. Lond. B* **353,** 131–140 (1998).
29. Sokal, R. R. & Rohlf, F. J. *Biometry* (W. H. Freeman, New York, 1995).
30. Parton, W. J. *et al.* Observations and modelling of biomass and soil organic matter dynamics for the grassland biome worldwide. *Glob. Biogeochem. Cycles* **7,** 785–809 (1993).

Acknowledgements We thank S. J. Brentnall for running the USCM simulations, P. J. Valdes for providing the Cretaceous GCM climate, W. G. Chaloner, L. J. Hickey, R. J. Norby, G. R. Upchurch, P. Wilf and F. I. Woodward for comments, and the Royal Society (D.J.B. and C.P.O.), the Leverhulme Trust (D.J.B.), the Natural Environmental Research Council, UK (D.J.B.), the US National Science Foundation (D.L.R.) and the US Department of Energy (R. A. Berner) for financial support.

Competing interests statement The authors declare that they have no competing financial interests.

Correspondence and requests for materials should be addressed to D.J.B. (d.j.beerling@sheffield.ac.uk).

Detoxification of vinyl chloride to ethene coupled to growth of an anaerobic bacterium

Jianzhong He*, Kirsti M. Ritalahti*, Kun-Lin Yang*, Stephen S. Koenigsberg† & Frank E. Löffler*‡

* *School of Civil and Environmental Engineering and*
‡ *School of Biology, Georgia Institute of Technology, Atlanta, Georgia 30332-0512, USA*
† *Regenesis Bioremediation Products, 1011 Calle Sombra, San Clemente, California 92672-6244, USA*

Tetrachloroethene (PCE) and trichloroethene (TCE) are ideal solvents for numerous applications, and their widespread use makes them prominent groundwater pollutants. Even more troubling, natural biotic and abiotic processes acting on these solvents lead to the accumulation of toxic intermediates (such as dichloroethenes) and carcinogenic intermediates (such as vinyl chloride)[1–4]. Vinyl chloride was found in at least 496 of the 1,430 National Priorities List sites identified by the US Environmental Protection Agency, and its precursors PCE and TCE are present in at least 771 and 852 of these sites, respectively[5]. Here we describe an unusual, strictly anaerobic bacterium that destroys dichloroethenes and vinyl chloride as part of its energy metabolism,

generating environmentally benign products (biomass, ethene and inorganic chloride). This organism might be useful for cleaning contaminated subsurface environments and restoring drinking-water reservoirs.

Crucial to the detoxification of chloroethene-contaminated sites is the complete reductive dechlorination of these contaminants to non-chlorinated end products such as ethene, or their oxidation to carbon dioxide (mineralization). Microbial growth linked to the mineralization of *cis*-dichloroethene (*cis*-DCE) and vinyl chloride (VC) occurs under aerobic conditions[6,7], but VC is generated frequently from polychlorinated ethenes in anoxic and reduced environments. Thus, an anaerobic process that leads to complete detoxification would be most effective in achieving bioremediation *in situ*. Substantial information describing bacteria that use polychlorinated ethenes as metabolic electron acceptors has accumulated[8,9] but the populations capable of complete reductive dechlorination have remained elusive. *Dehalococcoides ethenogenes* strain 195 (GenBank accession number AF004928.2) has been shown to dechlorinate PCE to ethene, but this organism failed to gain energy from VC, slowly producing ethene in a co-metabolic process[10]. To exploit the reductive dechlorination process for environmental cleanup, finding organisms that efficiently reduce VC to ethene is a priority.

Starting with a microcosm capable of dechlorinating PCE to ethene[11], we isolated a novel bacterium that used VC as a growth-supporting electron acceptor, thereby transforming this carcinogenic compound to the benign products ethene and inorganic chloride. The isolation procedure took advantage of the organism's ability to derive all its energy required for growth from the reduction of VC to ethene. Continued transfers over 4 years in mineral salts medium amended with VC, hydrogen and acetate yielded a non-methanogenic, ethene-producing culture. Dechlorination occurred with acetate as the sole electron donor, although at lower rates, apparently mediated in association with a syntrophic, acetate-oxidizing partner population[11,12]. Consecutive transfers without hydrogen achieved further enrichment of the dechlorinating population. VC dechlorination activity was recovered repeatedly from 10^{-5} dilutions of consecutive dilution-to-extinction series in hydrogen-amended medium. Microscopic examination after this enrichment procedure revealed the presence of three morphotypes: a small, disc-shaped organism and two rod-shaped organisms, one short and one long. Early attempts to tease out the VC-dechlorinating population in pure culture by using the dilution-to-extinction principle as well as cultivation in semisolid medium containing 0.5% low-melting agarose were unsuccessful. Similarly to *Dehalococcoides* strains 195 (ref. 10) and CBDB1 (ref. 13), the addition of high concentrations of the peptidoglycan inhibitor ampicillin did not prohibit dechlorination, and after five consecutive transfers in liquid medium with 1 mg ml^{-1} ampicillin, the rod-shaped organisms were no longer detectable by microscopic examination. After treatment with ampicillin, dechlorinating activity was recovered repeatedly from 10^{-7} dilutions in defined basal salts medium amended with VC, hydrogen and acetate. In addition, VC dechlorination occurred after transferring tiny opaque colonies that developed after 4–5 weeks in semisolid medium to liquid medium. No growth occurred in complex medium, and the culture seemed microscopically homogeneous (Fig. 1a). The isolate, designated BAV1, is a small non-motile organism of no more than 0.8 μm in diameter (Fig. 1). Careful light-microscopic analysis suggested that BAV1 cells are disc-shaped rather than coccoid, supporting an earlier observation indicating that *Dhc. ethenogenes* strain 195 cells might be flattened[10]. Cells suspended in liquid seemed to tumble end over end, a phenomenon explained by a disc-shaped morphology. High-resolution scanning electron microscopy also suggested that BAV1 cells have a disc-shaped rather than a coccoid morphology (Fig. 1b). Figure 1b,c shows individual BAV1 cells and features peculiar filamentous appendages on the cell's surface. Different 16S ribosomal RNA gene-based approaches corroborated

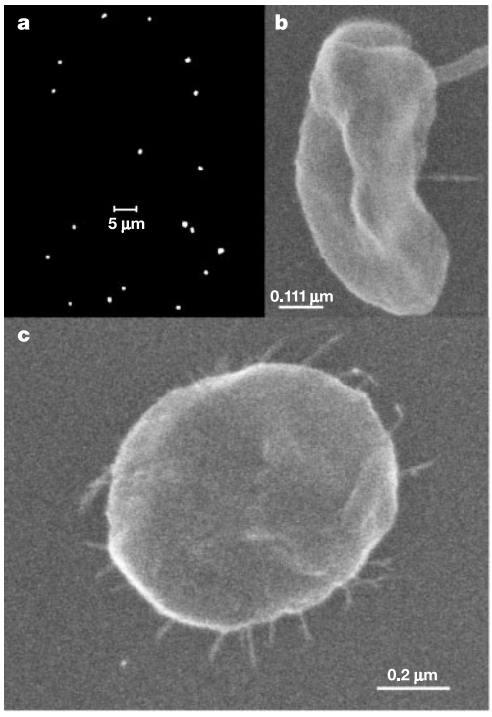

Figure 1 Micrographs of isolate BAV1. **a**, Epifluorescence observed after acridine orange staining. Original magnification × 1,000. **b**, **c**, Scanning electron micrographs indicating a disc-shaped morphology (**b**) and displaying peculiar appendages (**c**).

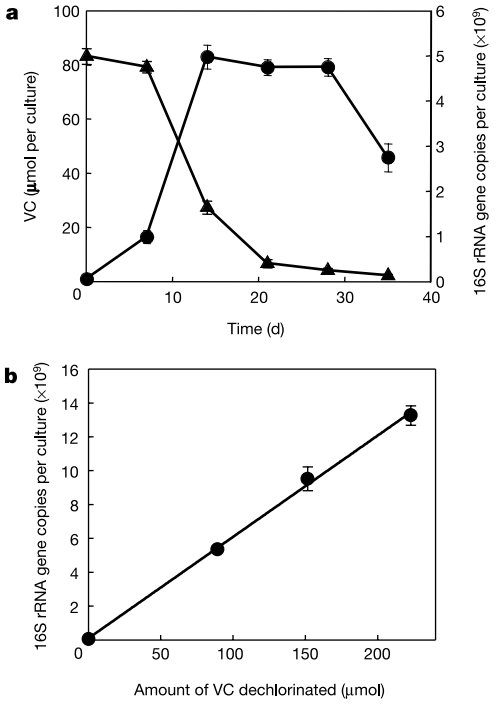

Figure 2 VC-dependent growth of isolate BAV1. **a**, An increase in 16S rRNA gene copies as determined by real-time PCR (circles) during the reductive dechlorination of VC (triangles) to ethene (not shown) by culture BAV1. **b**, 16S rRNA gene copies of isolate BAV1 after dechlorinating different amounts of VC. Data points were averaged from triplicates; error bars ± s.d. are not shown if they are hidden by the symbol.

Table 1 **Electron acceptor utilization profiles of defined *Dehalococcoides*-like populations**

Dehalococcoides sp.*	Reference	Electron acceptors
Dhc. ethenogenes strain 195 (C, AF004928.2)	10	PCE, TCE, *cis*-DCE, 1,1-DCE, 1,2-dichloroethane, 1,2-dibromoethane
Dhc. sp. strain VS (V, AF388550)†	15	*cis*-DCE, VC
Dhc. sp. strain FL2 (P, AF357918.2)	9	TCE, *cis*-DCE
Dhc. sp. strain BAV1 (P, AY165308)	This study	*cis*-DCE, *trans*-DCE, 1,1-DCE, VC, vinyl bromide, 1,2-dichloroethane
Dhc. sp. strain CBDB1 (P, AF230641)	13,25	1,2,3-TCB, 1,2,4-TCB, 1,2,3,4-TeCB, 1,2,3,5-TeCB, 1,2,4,5-TeCB, PCDD‡

*Group designations according to ref. 14: C, Cornell; V, Victoria; P, Pinellas sequence subgroups; also indicated are the GenBank accession numbers and references.
†Bacterium VS was identified in a mixed culture.
‡TCB, trichlorobenzene; TeCB, tetrachlorobenzene; PCDD, polychlorinated dibenzo-*p*-dioxins.

the purity of the culture. Terminal restriction-fragment-length polymorphism revealed single peaks of the expected sizes of 197, 442 and 512 base pairs (bp) after digestion of the amplicons with the restriction enzymes *Hha*I, *Msp*I and *Rsa*I, respectively. Denaturing gradient gel electrophoresis analysis yielded a single 148-bp band, whose sequence exactly matched that of isolate BAV1. Amplified ribosomal DNA restriction analysis (ARDRA) of 80 clones from two 16S rRNA gene clone libraries established with genomic DNA obtained from a VC-grown culture generated patterns predicted by digestion *in silico*, indicating that all 16S rRNA gene inserts contained in the clone libraries belonged to isolate BAV1. The fact that the *Dhc. ethenogenes* strain 195 genome (www.tigr.org) possesses a single ribosomal RNA operon suggested that a particular 16S rRNA gene-based analytical technique would not be complicated by the possible variations in multiple (slightly different) 16S rRNA gene sequences.

Isolate BAV1 respired VC in defined, completely synthetic basal salts medium amended with acetate and hydrogen (Fig. 2a). At room temperature (22–25 °C), BAV1 dechlorinated VC at up to $134.2 \pm 10\,\mathrm{nmol\,min^{-1}}$ per mg of protein, and grew with a doubling time of 2.2 days to yield 239 ± 27 mg (mean $\pm$ s.d., $n = 6$) of protein per mole of chloride released. Growth depended strictly on reductive dechlorination and the presence of hydrogen as an electron donor, which could not be replaced by organic substrates including formate, acetate, lactate, pyruvate, propionate, glucose, ethanol or yeast extract. Besides VC, other growth-supporting electron acceptors included *cis*-DCE, *trans*-DCE, 1,1-DCE or 1,2-dichloroethane and vinyl bromide; stoichiometric amounts of ethene accumulated as the reduced end product. It is notable that BAV1 is the first isolate capable of the metabolic dechlorination of all DCE isomers. Chlorinated compounds not supporting growth included PCE, TCE, chlorinated propanes, 1,1,1-trichloroethane, 1,1-dichloroethane and chloroethane. However, PCE and TCE were co-metabolized in the presence of a growth-supporting chloroethene and ethene was produced. Other organic and inorganic electron acceptors such as nitrate, fumarate, ferric iron, sulphite, sulphate, thiosulphate, sulphur or oxygen were not utilized, and no fermentative growth was observed. Respiratory growth was demonstrated conclusively by the chloroethene-dependent increase in cellular macromolecules (such as protein and DNA). Neither cell proliferation nor protein increase was detected in cultures lacking VC, acetate or hydrogen. Real-time polymerase chain reaction (PCR) showed that the increase in cell numbers was concomitant with the consumption of VC (Fig. 2a). A linear increase in biomass (that is, cells, as measured by the increase in 16S rRNA gene copies) occurred with increasing amounts of VC provided as electron acceptor, indicating a tight coupling between reductive dechlorination and growth (Fig. 2b). The number of 16S rRNA gene copies measured in cultures without VC corresponded to the number of cells transferred with the inoculum, confirming that no growth occurred in the absence of VC. Cultures that had consumed 80 μmol of *cis*-DCE contained about twice as many 16S rRNA gene copies than cultures grown with 80 μmol of VC (for example, $(9.28 \pm 0.41) \times 10^9$ copies versus $(4.99 \pm 0.26) \times 10^9$ copies). These findings show that BAV1 captured energy from both dechlorination steps when grown with *cis*-DCE.

Phylogenetic analysis, performed by using double-stranded 16S rRNA gene sequencing, affiliated isolate BAV1 (AY165308) with the Pinellas group of the *Dehalococcoides* cluster[14], a deep branch within the phylum Chloroflexi (green non-sulphur bacteria)[13]. The Pin-ellas group also includes *Dehalococcoides* sp. strains CBDB1 (AF230641)[13] and FL2 (AF357918.2)[9]. Metabolic ethene formation is not restricted to members of the Pinellas group and was described in a mixed culture containing a *Dehalococcoides* population of the Victoria group[15]. Table 1 shows known metabolic electron acceptors along with the phylogenetic grouping of identified *Dehalococcoides*-like populations. BAV1 shares a highly similar 16S rRNA gene sequence with *Dehalococcoides* populations that failed to dechlorinate chloroethenes or grow with VC as a metabolic electron acceptor (for example, strains CBDB1 and FL2). This high degree of 16S rRNA gene sequence similarity among members of the *Dehalococcoides* cluster implies that an analysis of 16S rRNA gene sequences cannot distinguish between populations of this group exhibiting different physiological activities. Hence, focusing only on 16S rRNA gene sequence analysis is not sufficient for characterizing the dechlorinating community or for the reliable prediction of the dechlorination potential associated with a particular environment.

Complete reductive dechlorination of chlorinated ethenes to non-toxic end products has been documented extensively in laboratory studies[12,15,16], and ethene formation was observed at some contaminated sites[14]. However, until now no organisms that efficiently dechlorinate VC have been obtained in pure culture. The isolation of the VC-respiring population BAV1 is a relevant milestone in chloroethene detoxification and provides deeper insight into poorly understood halogen cycles that involve the natural formation and utilization of chloroorganic compounds, including VC[17,18]. The comprehension of such cycles might explain why complete reductive dechlorination does not occur at all contaminated sites, even after alteration and optimization of geochemical conditions or supplying suitable electron donors to accelerate microbial activity. A recent pilot demonstration in a hydraulically controlled recirculation test plot at the chloroethene-contaminated Bachman Road site in Oscoda, Michigan, supports bioaugmentation with BAV1 as a promising approach to achieve detoxification at sites where the indigenous microbiota to drive the reductive dechlorination process to completion is absent or the rates of contaminant removal are insufficient[19]. Such innovative technologies are needed to clean up numerous chloroethene-contaminated aquifers at reasonable costs within acceptable time frames, and to protect threatened drinking-water reservoirs. □

Methods

Medium preparation

Completely defined, anaerobic mineral salts medium was prepared as described[12,20,21]. The enrichment and isolation process was performed in 20-ml glass vials containing 10 ml (final volume) of growth medium, whereas the cultures used for kinetic studies or molecular analyses were grown in 160-ml serum bottles containing 100 ml of medium. Unless indicated otherwise, cultures were incubated at 30 °C in the dark without shaking. Soluble substrates were added at 5 mM. Hydrogen was added by syringe to at least double

the concentration required for complete reductive dechlorination (namely 8.5–17 kPa). Chlorinated compounds were added to final aqueous concentrations in the range of 0.47–1.33 mM. Semisolid medium was prepared by adding 0.5% w/w low-melting agarose before autoclaving.

Analytical techniques

The protein content of liquid cultures was estimated as follows. Cells were harvested from 8 ml of culture fluid by centrifugation (10 min, 10,000 *g*). After alkaline cell lysis[22], the Coomassie Plus Protein Assay Reagent Kit (Pierce Biotechnology, Rockford, Illinois) was used in accordance with the manufacturer's recommendations. Spectrophotometric determination at 595 nm was used to quantify protein by comparing the sample absorbance with protein standards of known concentration prepared in the same way as the samples. Chloroethene and ethene concentrations were determined by gas chromatography as described[12].

Electron microscopy

A Zeiss LSM 510 confocal microscope with a Plan-Neofluar objective (100×; numerical aperture, 1.3) was used to obtain micrographs of cell suspensions after staining with acridine orange (15–60 min in 0.01% aqueous solution). Scanning electron microscopy micrographs were obtained with a TOPCON DS-130 field-emission scanning electron microscope with samples staged 'in-lens' and photographed at 20 kV. Samples were prepared as described[23], and coated with chromium (about 1.5 nm thickness) in a Denton DV-602 turbo magnetron sputter system.

Molecular analyses

DNA was extracted from actively growing cultures as described[12]. Real-time PCR to quantify BAV1 cells used a probe targeted to the *Dehalococcoides* 16S rRNA gene, tagged with a 6-carboxyfluorescein reporter fluorochrome on the 5′ end, and *N*,*N*,*N*′,*N*′-tetramethyl-6-carboxyrhodamine quencher on the 3′ end as described previously[12]. Linear calibration curves ($r^2 > 0.99$) were generated, spanning a template concentration range from 6.9×10^2 to 6.9×10^6 16S rRNA gene copies per 30-μl reaction volume by using BAV1 genomic DNA or plasmid DNA containing the 16S rRNA gene from BAV1. Analysis of individual clones with ARDRA was performed as described previously[12,24], except that the PCR-amplified 16S rRNA gene products from each clone were digested for 3 h with enzymes *Hha*I, *Msp*I and *Rsa*I at 37 °C. The reactions were terminated by incubation at 65 °C for 10 min, in accordance with the manufacturer's recommendations (Gibco), and the resulting fragments were resolved by electrophoresis for 2 h on 2.5% low-melting agarose gel (Seaplaque; Cambrex, Rockland, Maine). The fluorescently labelled primer 8F-hex (5′-AGA GTT TGA TCC TGG CTC AG-3′) and unlabelled 1492R (5′-GC(C/T) TAC CTT GTT ACG ACT T-3′) were used to amplify the 16S rRNA gene from pure culture DNA. Fluorescently labelled terminal fragments obtained by digesting the PCR product with *Hha*I, *Msp*I and *Rsa*I were analysed at Michigan State University's Genomics Technology Support Facility. Denaturing gradient gel electrophoresis was performed by Microbial Insights (Rockford, Tennessee) with the use of universal bacterial primers corresponding to *Escherichia coli* positions 341–534 as described[16].

Received 29 January; accepted 29 April 2003; doi:10.1038/nature01717.

1. Kielhorn, J., Melber, C., Wahnschaffe, U., Aitio, A. & Mangelsdof, I. Vinyl chloride: still a cause for concern. *Environ. Health Perspect.* **108,** 579–588 (2000).
2. Mohn, W. W. & Tiedje, J. M. Microbial reductive dehalogenation. *Microbiol. Rev.* **56,** 482–507 (1992).
3. Roberts, A. L. *et al.* Reductive elimination of chlorinated ethylenes by zero-valent metals. *Environ. Sci. Technol.* **30,** 2654–2659 (1996).
4. Vogel, T. M., Criddle, C. S. & McCarty, P. L. Transformation of halogenated aliphatic compounds. *Environ. Sci. Technol.* **21,** 722–736 (1987).
5. US Environmental Protection Agency. Agency for Toxic Substances and Disease Registry, ToxFAQs for chlorinated ethenes; www.atsdr.cdc.gov/tfacts70.html (1996).
6. Coleman, N. V., Mattes, T. E., Gossett, J. M. & Spain, J. C. Phylogenetic and kinetic diversity of aerobic vinyl chloride-assimilating bacteria from contaminated sites. *Appl. Environ. Microbiol.* **68,** 6162–6171 (2002).
7. Coleman, N. V., Mattes, T. E., Gossett, J. M. & Spain, J. C. Biodegradation of *cis*-dichloroethene as the sole carbon source by a β-Proteobacterium. *Appl. Environ. Microbiol.* **68,** 2726–2730 (2002).
8. Holliger, C., Wohlfarth, G. & Diekert, G. Reductive dechlorination in the energy metabolism of anaerobic bacteria. *FEMS Microbiol. Rev.* **22,** 383–398 (1998).
9. Löffler, F. E., Cole, J. R., Ritalahti, K. M. & Tiedje, J. M. in *Dehalogenation: Microbial Processes and Environmental Applications* (eds Häggblom, M. M & Bossert, I. D.) 53–87 (Kluwer Academic, New York, 2003).
10. Maymó-Gatell, X., Chien, Y.-T., Gossett, J. M. & Zinder, S. H. Isolation of a bacterium that reductively dechlorinates tetrachloroethene to ethene. *Science* **276,** 1568–1571 (1997).
11. He, J. *et al.* Acetate versus hydrogen as direct electron donors to stimulate the microbial reductive dechlorination process at chloroethene-contaminated sites. *Environ. Sci. Technol.* **36,** 3945–3952 (2002).
12. He, J., Ritalahti, K. M., Aiello, M. R. & Löffler, F. E. Complete detoxification of vinyl chloride (VC) by an anaerobic enrichment culture and identification of the reductively dechlorinating population as a *Dehalococcoides* population. *Appl. Environ. Microbiol.* **69,** 996–1003 (2003).
13. Adrian, L., Szewzyk, U., Wecke, J. & Görisch, H. Bacterial dehalorespiration with chlorinated benzenes. *Nature* **408,** 580–583 (2000).
14. Hendrickson, E. R. *et al.* Molecular analysis of *Dehalococcoides* 16S ribosomal DNA from chloroethene-contaminated sites throughout North America and Europe. *Appl. Environ. Microbiol.* **68,** 485–495 (2002).
15. Cupples, A. M., Spormann, A. M. & McCarty, P. L. Growth of a *Dehalococcoides*-like microorganism on vinyl chloride and *cis*-dichloroethene as electron acceptors as determined by competitive PCR. *Appl. Environ. Microbiol.* **69,** 953–959 (2003).
16. Duhamel, M. *et al.* Comparison of anaerobic dechlorinating enrichment cultures maintained on tetrachloroethene, trichloroethene, *cis*-dichloroethene and vinyl chloride. *Water Res.* **36,** 4193–4202 (2002).
17. Gribble, G. W. in *Chlorinated Compounds in the Biosphere, Natural Production* (ed. Meyers, R. A.) 972–1035 (Wiley, New York, 1998).
18. Keppler, F., Borchers, R., Pracht, J., Rheinberger, S. & Scholer, H. F. Natural formation of vinyl chloride in the terrestrial environment. *Environ. Sci. Technol.* **36,** 2479–2483 (2002).
19. Lendvay, J. M. *et al.* Bioreactive barriers: bioaugmentation and biostimulation for chlorinated solvent remediation. *Environ. Sci. Technol.* **37,** 1422–1431 (2003).
20. Löffler, F. E., Ritalahti, K. M. & Tiedje, J. M. Dechlorination of chloroethenes is inhibited by 2-bromoethanesulfonate in the absence of methanogens. *Appl. Environ. Microbiol.* **63,** 4982–4985 (1997).
21. Löffler, F. E., Tiedje, J. M. & Sanford, R. A. Fraction of electrons consumed in electron acceptor reduction and hydrogen threshold as indicators of halorespiratory physiology. *Appl. Environ. Microbiol.* **65,** 4049–4056 (1999).
22. Gerhardt, P. (ed.) *Manual of Methods for General Bacteriology* (American Society for Microbiology, Washington DC, 1981).
23. Sung, Y. *et al.* Characterization of two tetrachloroethene-reducing, acetate-oxidizing anaerobic bacteria and their description as *Desulfuromonas michiganensis* sp. nov. *Appl. Environ. Microbiol.* **69,** 2964–2974 (2003).
24. Löffler, F. E., Sun, Q., Li, J. & Tiedje, J. M. 16S rRNA gene-based detection of tetrachloroethene (PCE)-dechlorinating *Desulfuromonas* and *Dehalococcoides* species. *Appl. Environ. Microbiol.* **66,** 1369–1374 (2000).
25. Bunge, M. *et al.* Reductive dehalogenation of chlorinated dioxins by an anaerobic bacterium. *Nature* **421,** 357–360 (2003).

Acknowledgements Electron micrographs were obtained by R. P. Apkarian at the Integrated Microscopy and Microanalytical Facility at Emory University, Atlanta, Georgia. This work was supported by the Strategic Environmental Research and Development Program, and by a National Science Foundation CAREER award to F.E.L.

Competing interests statement The authors declare that they have no competing financial interests.

Correspondence and requests for materials should be addressed to F.E.L. (frank.loeffler@ce.gatech.edu).

Delta-wing function of webbed feet gives hydrodynamic lift for swimming propulsion in birds

L. Christoffer Johansson* & R. Åke Norberg†

** Department of Organismic and Evolutionary Biology, Harvard University, 26 Oxford Street, Cambridge, Massachusetts 02138, USA*
† Department of Zoology, Göteborg University, Box 463, SE-405 30 Göteborg, Sweden

Most foot-propelled swimming birds sweep their webbed feet backwards in a curved path that lies in a plane aligned with the swimming direction. When the foot passes the most outward position, near the beginning of the power stroke, a tangent to the foot trajectory is parallel with the line of swimming and the foot web is perpendicular to it. But later in the stroke the foot takes an increasingly transverse direction, swinging towards the longitudinal axis of the body. Here we show that, early in the power stroke, propulsion is achieved mostly by hydrodynamic drag on the foot, whereas there is a gradual transition into lift-based propulsion later in the stroke. At the shift to lift mode, the attached vortices of the drag-based phase turn into a starting vortex, shed at the trailing edge, and into spiralling leading-edge vortices along the sides of the foot. Because of their delta shape, webbed feet can generate propulsive forces continuously through two successive modes, from drag at the beginning of the stroke, all the way through the transition to predominantly lift later in the stroke.

Foot propulsion in swimming birds has generally been considered to be drag-based, both in surface swimming and during diving[1,2]. Drag is the hydrodynamic force that opposes movement